Mutations in *PRP43* That Uncouple RNA-Dependent NTPase Activity and Pre-mRNA Splicing Function†

Naoko Tanaka and Beate Schwer*

Department of Microbiology and Immunology, Weill Medical College of Cornell University, 1300 York Avenue, New York, New York 10021

Received December 30, 2005; Revised Manuscript Received March 8, 2006

ABSTRACT: *Saccharomyces cerevisiae* Prp43 is a DEAH-box RNA-dependent ATPase that catalyzes the release of excised lariat intron from the mRNA spliceosome. Previous studies identified mutations in Prp43 motifs I, II, and VI that were lethal in vivo and ablated ATP hydrolysis in vitro. Such Prp43 mutants exerted dominant-negative growth phenotypes when expressed in wild type cells and blocked intron release in vitro when added to yeast splicing extracts. Here, we assessed the effects of alanine and conservative substitutions at conserved residues in motifs Ia (^{146}TQPRRVAA^{153}), IV (^{307}LLFLTG^{312}), and V (^{376}TNIAETSLT^{384}) and thereby identified Arg150 (motif Ia), Phe309 (motif IV), Thr376, Leu383, and Thr384 (motif V) as being important for Prp43 function in vivo. Motif V mutations T376V, T384A, and T384V were lethal and dominant negative in vivo, and the mutant proteins inhibited lariat release in vitro. The T384A and T384V proteins were proficient for ATP hydrolysis, suggesting that ATPase activity is necessary, but not sufficient, for Prp43 function. We report that Prp43 hydrolyzes all common NTPs and dNTPs and unwinds short 5′/3′ tailed RNA/DNA duplexes in an ATP-dependent fashion. Optimal ATP hydrolysis requires an RNA cofactor of ≥20 nt. Prp43 is largely indifferent to mutations in its C-terminal segment, which is conserved in the DEAH-box splicing factors Prp2, Prp16, and Prp22.

Nucleic acid-dependent NTPases of the DExH/D box family are essential for remodeling the large RNP complexes that catalyze pre-mRNA splicing, ribosome biogenesis, and translation (*1*−*3*). DExH/D proteins are defined by a set of seven or eight conserved peptide motifs including the signature motif II, which can be DEAD, DEAH, or DExH (*4*−*6*). The repertoire of biochemical activities ascribed to DExH/D NTPases includes unwinding of nucleic acid duplexes, displacement of proteins from RNA, and annealing of RNA strands (*6*−*9*). It has been proposed that DExH/D proteins use the energy of NTP hydrolysis to modulate the structure or the composition of RNA−protein assemblies (*10*−*12*). However, the molecular mechanisms by which DExH/D proteins accomplish this and the conformational changes elicited by them are poorly understood.

The pre-mRNA spliceosome employs at least eight proteins of the DExH/D family (*3*). Prp5,[1] Prp28, Brr2, and Sub2/UAP56 are involved in assembling snRNPs and proteins onto the precursor RNA (*3*). Prp2 and Prp16 use NTP hydrolysis to drive the first and second transesterification reactions, respectively (*13*, *14*). Prp22 and Prp43 then act sequentially to release mature RNA and lariat intron from the spliceosome (*15*−*19*). Prp2, Prp16, Prp22, and Prp43 belong to the DEAH subgroup (*17*, *20*). They contain a central ATPase/helicase domain encompassing conserved motifs I−VI, and they also share a ∼300 amino acid C-terminal domain not found in other DExH/D proteins (*21*). Understanding how these DEAH paralogs carry out their distinct functions during the splicing cycle requires a detailed description of the enzymatic activities to highlight similarities and uncover differences.

The significance of conserved residues in motifs I (GxGKT), II (DEAH), III (SAT), and VI (QRxGRxGR) for viability and ATP hydrolysis has been tested for each of the spliceosomal DEAH box proteins in *Saccharomyces cerevisiae* (*18*, *22*−*27*). The salient point of these studies is that ATPase activity is necessary for the biological function and for splicing activity in each case.

Here, we further characterize the biochemical activities and structure−function relationships of *S. cerevisiae* Prp43, a 767-amino acid RNA-dependent ATPase that releases the excised lariat intron from the spliceosome. We show that Prp43 hydrolyzes all common NTPs and dNTPs and that it disrupts short nucleic acid duplexes in an NTP-dependent fashion. We assess the effects of alanine substitutions at conserved residues in motifs Ia (^{146}TQPRRVAA^{153}), IV (^{307}LLFLTG^{312}), and V (^{376}TNIAETSLT^{384}). We show that lethal mutations at position Thr384 (motif V) uncouple ATPase activity from Prp43's role in releasing lariat intron RNA from the spliceosome. These findings suggest that ATPase activity is not sufficient for the biological function of Prp43.

† This work was supported by NIH Grant GM50288.

* Corresponding author. Mailing address: Department of Microbiology and Immunology, Weill Medical College of Cornell University, 1300 York Avenue, New York, NY 10021. Tel: (212) 746−6518. Fax: (212) 746-8587. E-mail: bschwer@med.cornell.edu.

[1] Abbreviations: Prp, precursor RNA processing; pre-mRNA, precursor messenger RNA; Tris, tris(hydroxymethyl)aminomethane; DTT, dithiothreitol; EDTA, (ethylenedinitrilo)tetraacetic acid; SDS, sodium dodecyl sulfate; PAGE, polyacrylamide gel electrophoresis; BSA, bovine serum albumin; NTP, nucleoside triphosphate; AMPPCP, β,γ-methyleneadenosine 5′-triphosphate; bp, base pair(s); nt, nucleotide(s).

10.1021/bi052656g CCC: $33.50 © 2006 American Chemical Society
Published on Web 04/29/2006

Prior deletion analyses showed that the conserved C-terminal segments are important for the biological functions of the DEAH splicing factors Prp2, Prp16, Prp22, and Prp43 (*18*, *21*, *23*, *28*, *29*). In the case of Prp2, the C-terminal domain is required for spliceosome binding through interaction with Spp2 (*30*). Here, we introduced single-alanine or alanine-cluster mutations at 97 residues within the C-terminal domain. None of the *PRP43* alleles was lethal, suggesting that individual conserved residues within the C-domain are not critical for Prp43 function in vivo.

MATERIALS AND METHODS

Targeted Mutagenesis and Analysis of Prp43 Mutants in Vivo. Mutations were introduced into the *PRP43* gene using the two-stage PCR overlap extension method as described (*18*). The mutated DNA fragments were inserted into p358-PRP43 (*TRP1 CEN*) in lieu of the wild type gene. The plasmids carrying the mutant alleles were transformed into the *prp43*Δ strain (Mat**a** *ura3-52 trp1-63 his3-*Δ*200 leu2-1 ade2-101 lys2-801 prp43::kanMX*) containing *PRP43* on a *CEN URA3* plasmid. Trp^+ transformants were selected and streaked to 5-FOA medium to select cells that had lost the *PRP43 URA3* plasmid. The ability of the mutant alleles to support growth on 5-FOA was assessed at 19, 30, and 37 °C.

Expression and Purification of Prp43 Proteins. The open reading frames encoding wild type Prp43 or the T376A, T376V, T376S, T384A, T384V, and T384S mutants were amplified by PCR and inserted into pET28-His_{10}Smt3 (a gift from Dr. Christopher Lima). The pET28-His_{10}Smt3-Prp43 plasmids were transformed into *Escherichia coli* BL21-Codon Plus (DE3) (Stratagene). Cultures were inoculated from single colonies and maintained in logarithmic growth at 37 °C in LB medium containing 50 μg/mL kanamycin to a final volume of 200 mL (1 L for T376V). When A_{600} reached 0.6−0.8, the cultures were chilled on ice for 30 min, IPTG was added to a final concentration of 0.4 mM, and the cultures were incubated for 16 h at 17 °C with constant shaking. Cells were harvested by centrifugation and stored at −20 °C.

The following procedures were carried out at 4 °C. Cell pellets were suspended in 20 mL of buffer A (50 mM Tris-HCl, pH 7.4, 250 mM NaCl, 10% sucrose), and lysozyme was added to 0.2 mg/mL. The suspension was mixed gently for 40 min, adjusted to 0.1% Triton X-100, and mixed further for 15 min. The suspension was sonicated to reduce viscosity, and insoluble material was then removed by centrifugation at 20000*g* for 30 min. The soluble lysate was mixed for 1 h with 5 mL (50% slurry) of Ni-NTA agarose (Qiagen) that had been equilibrated in buffer A. The resin was recovered by centrifugation and resuspended in buffer A (5 mL). The cycle of centrifugation and resuspension was repeated three times. The washed resin was again suspended in buffer A and poured into a column. Bound polypeptides were eluted stepwise with 25, 50, 100, 150, 200, and 300 mM imidazole in buffer E (50 mM Tris-HCl pH 7.4, 250 mM NaCl, 10% glycerol). Peak fractions containing His_{10}Smt3-Prp43 proteins (20−35 mg) were pooled and incubated for 1 h with the protease Ulp1 (20−35 μg). The solutions were cleared by centrifugation and concentrated using Amicon Ultra15 filters (Millipore). Aliquots were applied to a 320 mL HiLoad Superdex 200 column (Amersham) equilibrated in buffer D (50 mM Tris-HCl pH 7.4, 2 mM DTT, 1 mM EDTA, 10% glycerol) containing 150 mM NaCl, and proteins were eluted with the same buffer at a flow rate of 2.0 mL/min. Peak fractions containing Prp43 proteins (~24 mL) were pooled and mixed with heparin sepharose (5 mL of a 50% slurry) that had been equilibrated in buffer D containing 150 mM NaCl. The resin was collected, washed twice with buffer D containing 150 mM NaCl, and poured into a column. Bound proteins were eluted with 500 mM NaCl in buffer D. The polypeptide compositions of each fraction were monitored by SDS−PAGE and staining with Bio-Safe Coomassie dye (Bio-Rad). Protein concentrations were determined using the Bio-Rad dye-binding reagent with BSA as the standard. The yields from 200 mL cultures were 6.8 mg (wild type Prp43), 2.3 mg (T376A), 1.6 mg (T376S), 5.1 mg (T384A), 4.5 mg (T384V), and 5.4 mg (T384S). The yield of T376V protein, purified from a 1 L culture, was 1.3 mg.

NTPase Assays. NTPs were premixed with equimolar amounts of $MgCl_2$. Reaction mixtures (100 μL) contained 40 mM Tris-HCl (pH 8.0), 2 mM DTT, 1 mM NTP-Mg, and RNA and protein as indicated. Reaction mixtures were incubated for 2−60 min at 30 °C and quenched by addition of 1 mL of Biomol Green reagent (Biomol Research Laboratories, Plymouth Meeting PA), and the absorbance (A_{620}) was measured after 20 min at 23 °C. The amounts of free phosphate were calculated by interpolation of the A_{620} values to a phosphate standard curve. Kinetic parameters were determined by Lineweaver−Burk plots using the EnzymeKinetics program (Trinity Software). All values are averages from at least two measurements.

To determine the basal ATPase activities, Prp43 proteins (500 nM) were preincubated with RNase A (10 μg/mL) for 30 min at 30 °C and then added to the reaction mixtures. For measurements of stimulated ATP hydrolysis, poly(A) (Amersham) or RNA oligomers of defined length were added. The concentrations for poly(A) RNA are given as the concentration of nucleotides. RNA oligomers $(A)_{40}$, $(A)_{30}$, $(A)_{20}$, and $(A)_{10}$, RNA_{40} (5′-GCCGCCGUUCUCCUGGAUC-CAUAGGCACUGAGUUGGUAUG-3′), RNA_{30} (5′-UC-CUGGAUCCAUAGGCACUGAGUUGGUAUG-3′), and RNA_{20} (5′-AUAGGCACUGAGUUGGUAUG-3′) were purchased from Dharmacon. RNA concentrations are specified as the molarity of each oligonucleotide.

RNA Binding by Gel Mobility Shift Assays. Reaction mixtures (20 μL) containing 40 mM Tris-HCl (pH 8.0), 2 mM DTT, 2 nM 5′-^{32}P-labeled RNA, and Prp43 as specified were incubated for 30 min at 30 °C. Mixtures were transferred to ice and adjusted to 10% glycerol and 0.04% Triton X-100, and the products were separated by electrophoresis through an 8% polyacrylamide gel containing 20 mM Tris-borate, 0.25 mM EDTA. The ^{32}P-labeled RNA was visualized by exposure of the dried gel to film and quantified using a phosphorimager and ImageQuant (Molecular Dynamics).

Unwinding Assays. The 3′ and 5′ tailed RNA-DNA substrates were prepared as described (*31*). In brief, a 99 nt RNA strand (5′-GGGCGAAUUGGGCCCUCUAGAUGC-AUGCUCGAGCGGCCGCCAGUGUGAUGGAUAUCUGC-AGAAUUCGCCCUUAAACCAUAAUCAUACCAGUUUU-GGCAG-3′) was synthesized by in vitro transcription, and it was annealed at a 1:3 molar ratio of RNA:DNA to the 5′

^{32}P-labeled DNA oligonucleotides 5′-CATCACACTGGCGGCCGCTC to generate a 3′/5′ tailed 20 bp duplex, 5′-GAGCATGCATCTAGAGGGCCCAATTCGCCC to yield a 3′ tailed 30 bp duplex, and 5′-CTGCCAAAACTGGTATGATTATGGTTTAAG to yield a 5′ tailed 30 bp duplex. The annealed duplex substrates were gel-purified by native PAGE. The relative stabilities of the helicase substrates, determined according to the nearest neighbor method (*32*), were −33.6 kcal/mol (20 bp duplex), −48.6 kcal/mol (3′ tailed 30 bp duplex), and −34.6 kcal/mol (5′ tailed 30 bp duplex). Reaction mixtures (20 μL) containing 40 mM Tris-HCl (pH 7.0), 2 mM DTT, 1 mM ATP-Mg, 1.25 nM RNA/DNA substrate, and 1 μM Prp43 were incubated at 37 °C. Reactions were halted by transfer to ice and addition of 5 μL of loading buffer (100 mM Tris-HCl, pH 7.4, 5 mM EDTA, 0.5% SDS, 50% glycerol), 0.1% (w/v) bromophenol blue, and xylene cyanol dyes. Samples were analyzed by electrophoresis through an 8% polyacrylamide gel in 40 mM Tris-borate, 0.5 mM EDTA, 0.1% SDS. The ^{32}P-labeled substrate and products were visualized by autoradiography of the dried gel and quantified using a phosphorimager. The extent of unwinding (single-strand/total nucleic acid) in the presence of Prp43 was corrected for the background level of single-strand/total nucleic acid in the absence of protein. The background values varied from 8% to 14% in different experiments.

RESULTS

Conserved Amino Acids in Motifs Ia, IV, and V Are Important for Prp43 Function in Vivo. A prior study had shown that 5 alanine mutations at conserved residues within motifs I (^{119}GSGKT^{123}), II (^{215}DEAH^{218}), and VI (^{423}QRAGRAGR^{430}) that abolished ATPase activity in vitro were lethal in vivo, indicating that ATP hydrolysis is necessary for the biological function of Prp43 (*18*). Here we evaluated the role of 16 conserved amino acids in motifs Ia (^{146}TQPRRVAA^{153}), IV (^{307}LLFLTG^{312}), and V (^{376}TNIAETSLT^{384}) by alanine scanning (Figure 1). *PRP43-Ala* alleles were placed on *CEN TRP1* plasmids under the transcriptional control of the natural *PRP43* promoter, and their in vivo function was tested in a *prp43*Δ strain using the plasmid shuffle technique. Growth of a *prp43*Δ strain is contingent on a *PRP43 CEN URA3* plasmid. Trp$^+$ transformants were selected and then tested for growth on medium containing 5-FOA, a drug that selects against cells with the *URA3 PRP43* plasmid. Wild type *PRP43* and the mutant alleles *T146A*, *Q147A*, *P148A*, *R149A*, *R150A*, *L307A*, *F309A*, *T311A*, *G312A*, *T376A*, *N377A*, *E380A*, *T381A*, *S382A*, and *L383A* supported growth of the *prp43*Δ strain under 5-FOA selection at one or more of the temperatures tested (19, 30, 37 °C). In contrast, cells containing *T384A* did not form colonies on 5-FOA medium at 19, 30, or 37 °C, indicating that substitution of Thr384 in motif V by alanine abolished the function of Prp43 in vivo. The viable mutants were tested for growth on rich medium (YPD agar) at 14, 25, 30, and 37 °C. The *T376A* strain formed pinpoint colonies at all temperatures tested (Figure 1B). *R150A* (motif Ia) and *L383A* (motif V) displayed cold sensitive growth phenotypes. *F309A* (motif IV) failed to grow at 37 °C (Figure 1B).

We tested the effects of conservative substitutions at Thr376 and Thr384, positions in motif V at which alanine substitutions resulted in a severe growth defect or lethality.

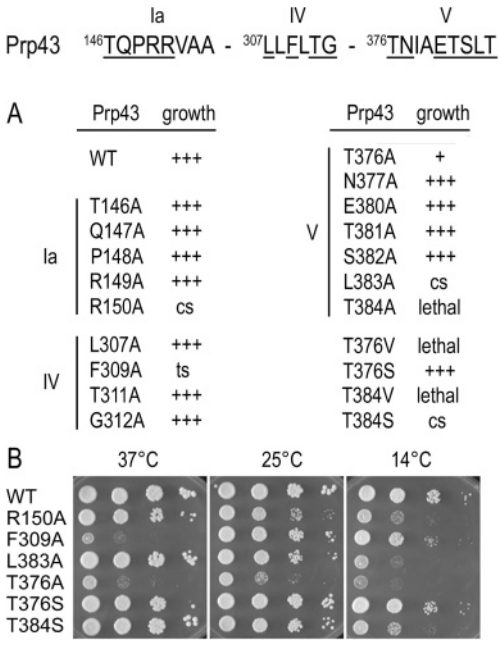

FIGURE 1: Mutational analysis of motifs Ia, IV, and V. The amino acid sequences of Prp43 motifs Ia, IV, and V are shown at the top. The numbers refer to the residues in Prp43; the positions that were replaced by alanine are underlined. (A) Summary of mutational effects. The ability of the various *PRP43* alleles to complement a *prp43*Δ strain was tested by plasmid shuffle. Alleles that did not complement the *prp43*Δ strain under 5-FOA selection are indicated by "lethal". Viable mutants were plated to rich medium (YPD) and incubated at 14, 25, 30, and 37 °C. Growth was scored based on colony size. +++ indicates growth comparable to that of wild type Prp43; + denotes slow growth at all temperature; cs and ts indicate a conditional growth phenotype at 14 and 37 °C, respectively. (B) *prp43*Δ cells carrying wild type *PRP43* (WT) or the indicated mutants were grown in liquid medium at 30 °C. The A_{600} was adjusted to 0.1, and aliquots (3 μL) of serial 10-fold dilutions were spotted onto YPD agar medium. The plates were photographed after incubation for 2 days at 37 °C, 3 days at 25 °C, and 6 days at 14 °C.

Whereas *T376S* and *T384S* cells were viable under 5-FOA selection, *T376V* and *T384V* cells failed to form colonies. We surmise that a side chain hydroxyl is critical at positions 376 and 384. *T376S* cells grew as well as wild type *PRP43* on YPD agar. *T384S* cells formed smaller colonies at 14 °C (Figure 1B), indicating that the additional methyl group present in threonine at position 384 is advantageous at low temperatures.

ATP Hydrolysis by Wild Type and Mutant Prp43 Proteins. To better define the biochemical properties of Prp43 and to determine the basis for the growth defects elicited by mutations in motif V, we produced His_{10}-Smt3-tagged wild type Prp43 and mutant proteins T376A, T376V, T376S, T384A, T384V, T384S in bacteria and isolated them from soluble bacterial lysates by nickel-agarose chromatography. The N-terminal His_{10}-Smt3 tag was removed by cleavage with the protease Ulp1 and separated from native Prp43 by gel filtration. The Prp43 proteins were then purified further by heparin sepharose chromatography. The predominant species in each preparation was the ~88 kDa Prp43 protein (Figure 2A).

ATP hydrolysis by wild type Prp43 depends on an RNA cofactor such as poly(A) (*18*). From the dependence of P_i release (from 1 mM ATP) on the concentration of poly(A), we determined a K_m for the RNA cofactor of 1.9 μM and a

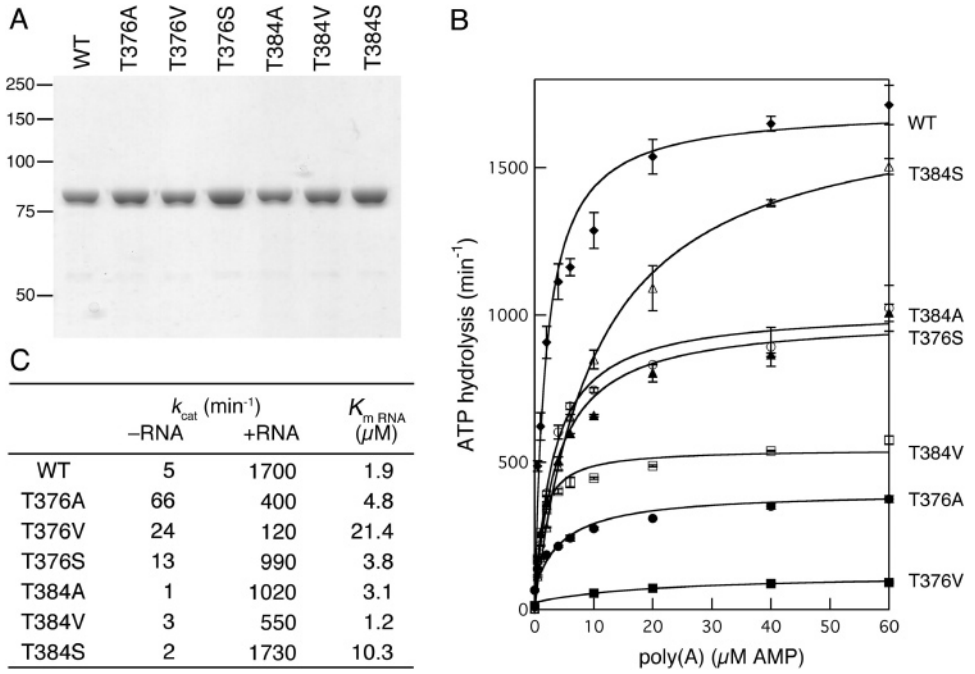

C

	k_{cat} (min^{-1}) –RNA	k_{cat} (min^{-1}) +RNA	$K_{m\ RNA}$ (μM)
WT	5	1700	1.9
T376A	66	400	4.8
T376V	24	120	21.4
T376S	13	990	3.8
T384A	1	1020	3.1
T384V	3	550	1.2
T384S	2	1730	10.3

FIGURE 2: RNA-dependent ATPase activity. (A) Prp43 proteins (1 μg) were separated by 8% SDS−PAGE and visualized by Coomassie staining. The positions and sizes (in kilodaltons) of marker proteins are indicated at the left. (B) P_i release was measured at 1 mM ATP-Mg and 0−60 μM of poly(A) (measured as AMP concentration). ATP hydrolysis (min^{-1}) of wild type Prp43 (WT) (◆); T384S (△); T384A (○); T376S (▲); T384V (□); T376A (●); T376V (■) was plotted as a function of poly(A) concentration. Each datum represents the average of two measurements; the error bars indicate the deviation from the average. (C) Summary of the ATPase activities. (−RNA): ATP hydrolysis (min^{-1}) was determined for the Prp43 proteins (50 nM) during 60 min incubations in the presence of RNase A. (+RNA): k_{cat} values were determined from Lineweaver−Burk plots of the curves shown in panel B using the EnzymeKinetics Program (Trinity Software). The K_m values for poly(A) RNA was determined from the Lineweaver−Burk plot of the data shown in panel B. ATP hydrolysis of T376V was measured at 0−500 μM poly(A).

turnover number of 1700 min^{-1} (Figure 2B,C). Parallel analyses of ATP hydrolysis by the Prp43 mutants showed that they had similar dependence on poly(A), but varied in their level of activity at saturating RNA concentrations (Figure 2B). The K_m values of T376A, T376S, T384A, and T384V proteins were 4.8, 3.8, 3.1, and 1.2 μM, respectively (Figure 2C), indicating that these mutations did not significantly affect the affinity for the RNA cofactor, vis-à-vis wild type Prp43. The K_m values of T384S and T376V for poly(A) were 10.3 and 21.4 μM, respectively, which are ~5- and 10-fold higher than that of wild type Prp43.

The k_{cat} values of wild type Prp43 and the viable T376S and T384S mutants were 1700, 990, and 1730 min^{-1} respectively. T376A, which elicited a severe constitutive growth defect (Figure 1B), had a k_{cat} of 400 min^{-1}. The turnover number of the lethal T376V mutant was 120 min^{-1}, i.e., 7% of wild type activity. The ATPase activities of the lethal T384A and T384V mutants were 1020 and 550 min^{-1}, or 60% and 32% of wild type activity, respectively. Because viable Prp43 mutants with as little as ~25% of wild type ATPase activity have been described here and previously (*18*), we surmise that T384A and T384V are lethal, not because of their reduced ATPase activity, but rather because they are defective for coupling the energy of ATP hydrolysis to a downstream event (see below).

ATP hydrolysis by wild type Prp43 and the motif V mutants was measured in the absence of exogenous RNA and in the presence of RNase A, which was added to eliminate the possibility that the protein preparations contained contaminating *E. coli* RNA. The RNA-independent ATPase activity of wild type Prp43 was 5 min^{-1}, which was lower by a factor of 340 than the RNA-dependent ATPase activity. The basal ATPase activities of T384A (1 min^{-1}), T384V (3 min^{-1}), and T384S (2 min^{-1}) were slightly below that of wild type. In contrast, the RNA-independent ATPase activities of T376A, T376V, and T376S were 66, 24, and 13 min^{-1}, representing a gain-of-function in the absence of cofactor (Figure 2C).

Effect of RNA Length on ATP Hydrolysis by Wild Type Prp43. ATP hydrolysis (at 1 mM ATP-Mg) was measured as a function of increasing concentrations of homooligomers $(A)_{40}$, $(A)_{30}$, $(A)_{20}$, $(A)_{10}$ and of oligonucleotides RNA_{40}, RNA_{30}, and RNA_{20} composed of mixtures of all 4 ribonucleotides (Figure 3). The k_{cat} values for the homopolymers were 1340 min^{-1} for $(A)_{40}$, 980 min^{-1} for $(A)_{30}$, 990 min^{-1} for $(A)_{20}$, and 290 min^{-1} for $(A)_{10}$. The k_{cat} values for the mixed oligomers were 1110 min^{-1} (RNA_{40}), 1050 min^{-1} (RNA_{30}), and 960 min^{-1} (RNA_{20}). The K_m values for $(A)_{40}$, $(A)_{30}$, $(A)_{20}$, and $(A)_{10}$ were 75, 150, 360, and 3200 nM, respectively (Figure 3A,C). For RNA_{40}, RNA_{30}, and RNA_{20}, the K_m values were 23, 46, and 100 nM (Figure 3B,C). These results indicate that the chain length influences the affinity of Prp43 for the RNA cofactor and, more modestly, the maximum stimulation of ATP hydrolysis.

Activation of Prp43 Mutants by RNA_{40}. ATP hydrolysis by T376A, T376S, T384A, and T384S mutants was measured in the presence of increasing concentrations of RNA_{40} (Figure 4). The k_{cat} values for T376A, T376S, T384A, and T384S were 500, 360, 350, and 910 min^{-1}, respectively (Figure 4B). The K_m values of the mutants for RNA_{40} were 23 nM (T376A), 17 nM (T376S), 20 nM (T384A), and 41 nM (T384S) (Figure 4B). These values were comparable to the

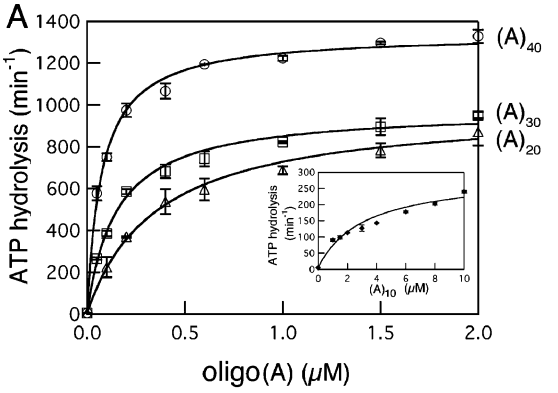

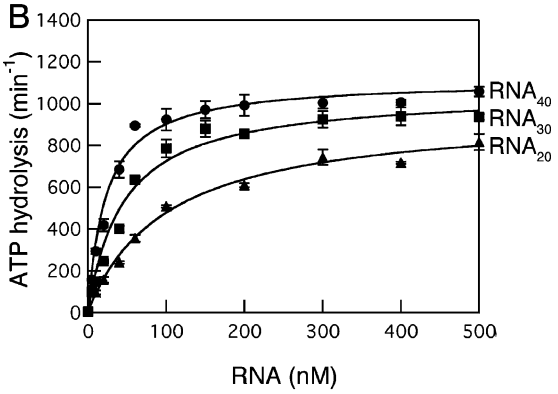

C

	k_{cat} (min^{-1})	$K_{m\ RNA}$ (nM)
$(A)_{40}$	1340	75
$(A)_{30}$	980	150
$(A)_{20}$	990	360
$(A)_{10}$	290	3200
RNA_{40}	1110	23
RNA_{30}	1050	46
RNA_{20}	960	100

FIGURE 3: Effect of RNA length. (A) ATPase activity (min^{-1}) was measured as a function of 0−2 μM homooligomers of 40 (○), 30 (□), and 20 (△) adenylates. The concentrations of Prp43 and ATP-Mg were 50 nM and 1 mM, respectively. The inset shows ATP hydrolysis as a function of 0−10 μM $(A)_{10}$. Each datum represents the average of two measurements; the error bars indicate the deviation from the average. (B) ATP hydrolysis was measured at 50 nM Prp43 and 1 mM ATP-Mg in the presence of increasing concentrations (0−500 nM) of mixed RNAs of 40 (●), 30 (■), and 20 (▲) nucleotides in length. (C) Summary. k_{cat} (min^{-1}) and K_m values were determined from Lineweaver−Burk plots of the data shown in panels A and B.

K_m for RNA_{40} of wild type Prp43 (23 nM) (Figure 3C) and paralleled the results for poly(A) (Figure 2B), thereby indicating that the motif V mutations had no grave effect on binding the RNA cofactor required for ATP hydrolysis.

RNA Binding. To assess the RNA binding capacity of Prp43 directly, we incubated 5′-labeled $(A)_{40}$, $(A)_{30}$, and $(A)_{20}$ with increasing concentrations of Prp43 (0.5−1000 nM) and analyzed the products by native PAGE (Figure 5). Inclusion of protein resulted in the appearance of RNA−protein complexes that migrated more slowly than the free RNA in native gels, in a discrete band (marked by an asterisk (*)) and in a smear (marked by a bar). We consider the appearance of a discrete RNA−protein complex to be indicative of stable RNA binding, whereas the smear likely

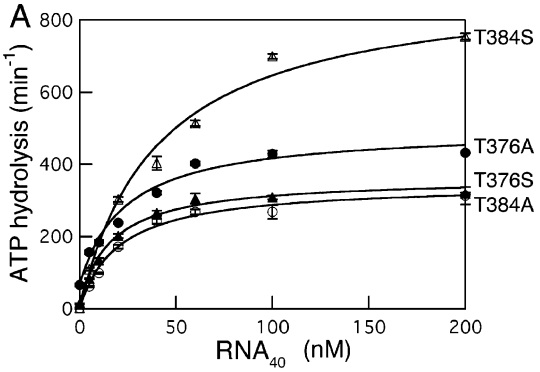

B

	k_{cat} (min^{-1})	$K_{m\ RNA}$ (nM)
T376A	500	23
T376S	360	17
T384A	350	20
T384S	910	41

FIGURE 4: RNA_{40}-stimulated ATP hydrolysis by Prp43 mutants. (A) ATP hydrolysis at 1 mM ATP-Mg was measured as a function of increasing concentrations (0−200 μM) of RNA_{40} for T384S (△), T376A (●), T376S (▲), and T384A (○). Each datum represents the average of two measurements; the error bars indicate the deviation from the average. (B) k_{cat} (min^{-1}) and K_m values for RNA_{40} were determined from Lineweaver−Burk plots of the data shown in panel A.

indicates that the Prp43−RNA complex dissociated during electrophoresis. We estimated K_d values (the protein concentration at which 50% of the RNA was bound) of 15 and 20 nM for $(A)_{40}$ and $(A)_{30}$, respectively. Prp43 formed very little stable complex with $(A)_{20}$; the majority of the signal was detected in a smear migrating above free RNA (Figure 5). The apparent K_d values for RNAs composed of all 4 nucleotides were 2 nM for RNA_{40} and 3 nM for RNA_{30} (Figure 6A). Prp43 did not bind to a 40-mer DNA of sequence identical to that of RNA_{40} (not shown).

^{32}P-labeled RNA_{40} was incubated with 1, 10, and 100 nM of Prp43 mutants T376A, T376V, T376S, T384A, T384V, and T384S, and the products were analyzed by native PAGE (Figure 6B). Mutations at Thr384 did not affect the RNA binding capacity of Prp43, and at 1 nM protein, ∼50% of RNA_{40} migrated as a discrete species near the top of the gel. At 100 nM protein, all of the RNA_{40} appeared in complexes that migrated slightly above those formed at lower protein concentrations. T376A, T376V, and T376S mutants did not form stable complexes; at protein concentrations of 10 and 100 nM, the majority of the labeled RNA migrated more slowly than the free probe, but not as a discrete species. Thus, mutations at Thr376 of Prp43 diminish the ability to form stable RNA−protein complexes in vitro. Because T376S and, to a lesser extent, T376A were functional in vivo, we infer that stable RNA binding in vitro is not critical for Prp43 function in vivo. Furthermore, the mutational effects on stable RNA binding assessed by native PAGE in vitro do not correlate with the RNA cofactor binding results for ATPase activation (Figures 2 and 4). We regard the RNA K_m value for ATPase activation as the more relevant parameter in interpreting the mutational outcomes.

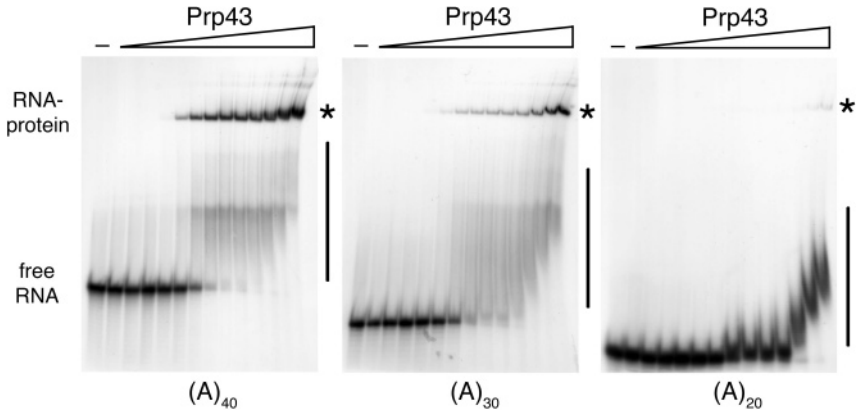

FIGURE 5: RNA binding. Reaction mixtures containing the indicated ^{32}P-labeled RNA and increasing concentrations (0.5, 1, 2, 5, 10, 20, 40, 60, 80, 100, 200, 500, and 1000 nM) of Prp43 were incubated for 30 min at 30 °C. Protein was omitted in the first lane (−) of each panel. The products were analyzed by native PAGE. Autoradiograms of the dried gels are shown. The positions for free RNA and stable RNA−protein complexes (*) are indicated. The bar denotes complexes that possibly dissociate during electrophoresis.

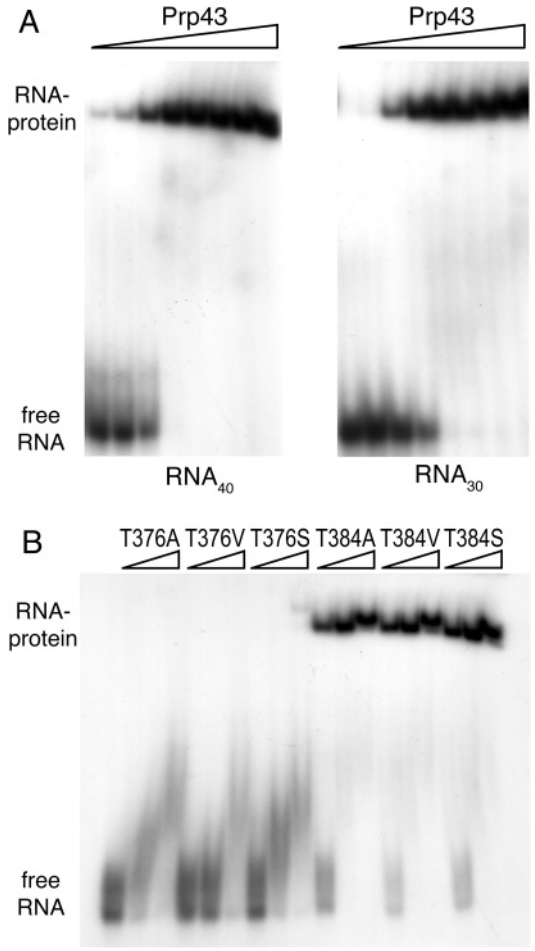

FIGURE 6: RNA binding. (A) ^{32}P-labeled RNA_{40} and RNA_{30} were incubated with increasing concentrations of Prp43 (0.5, 1, 2, 5, 10, 20, 50, and 100 nM) and analyzed by native PAGE. (B) ^{32}P-labeled RNA_{40} was incubated with 1, 10, and 100 nM of the indicated mutant proteins, and the products were analyzed by native PAGE. Autoradiograms of the dried gels are shown.

RNA Unwinding Activity of Prp43. Prp43 could disrupt a 20-bp RNA/DNA duplex containing single-stranded 5′ and 3′ RNA tails, albeit only under conditions of vast enzyme excess over substrate (Figure 7A). When the helicase substrate (1.25 nM) was incubated with Prp43 (1 μM) for 1 h at 37 °C in the presence of ATP and Mg^{2+}, nearly all of the labeled 20-mer was displaced and migrated ahead of the double-stranded substrate in an SDS-containing polyacrylamide gel. When ATP was omitted, or when the nonhydrolyzable ATP analogue AMPPCP was included, the single-stranded species comprised 10% of the total labeled RNA. AMPPCP inhibited ATP-dependent unwinding, insofar as the amount of single-stranded product was reduced to 18% in reactions that contained ATP plus AMPPCP, indicating that Prp43 could bind the nonhydrolyzable analogue. Thus, ATP hydrolysis is required for the unwinding activity of Prp43.

In the presence of Prp43 and ATP, the single-stranded product accumulated steadily over time, comprising 40% of the total labeled material at 10 min and 90% at 45 min (Figure 7A). Using RNA/DNA duplexes that contained either 3′ or 5′ single-stranded RNA tails, we found that Prp43 did not exhibit a strict directionality for unwinding, but that it could act on substrates with 5′ or 3′ overhangs (Figure 7B). The apparent preference for a 5′ tail was also observed when RNA/DNA duplexes of similar stability were used (not shown).

Mutants T384A, T384V, and T384S displaced 81%, 69%, and 85% of the 20-bp 5′/3′ tailed RNA/DNA duplex during 60 min incubations at 37 °C (Figure 7C; values corrected for background). In contrast, mutations at position Thr376 of Prp43 diminished the protein's ability to displace a short duplex; the amounts of single-stranded product after 1 h incubation were 8% (T376A, T376V) and 39% (T376S). Thus, the ability of a Prp43 mutant to unwind short duplex nucleic acids in vitro (Figure 7C) did not correlate with its activity in vivo (Figure 1B).

Nucleoside Triphosphate Specificity. P_i release by Prp43 was measured at 1 mM NTP/dNTP in the presence of saturating poly(A) (Figure 7C). The turnover numbers were similar for each of the nucleotides tested, and they ranged from 1020 min^{-1} for dCTP to 2420 min^{-1} for dTTP. We found that all NTPs and dNTPs supported Prp43-dependent unwinding of the 20-bp 5′/3′ tailed RNA/DNA duplex (not shown).

Overexpression of T376V, T384A, and T384V Elicit Dominant-Negative Phenotypes. Previous work showed that overexpression of lethal, ATPase-deficient Prp43 mutants (e.g. T123A in motif I) inhibited growth of wild type cells (*18*). To test whether the lethal *T376V*, *T384A*, and *T384V* mutants interfered with the function of wild type Prp43, we

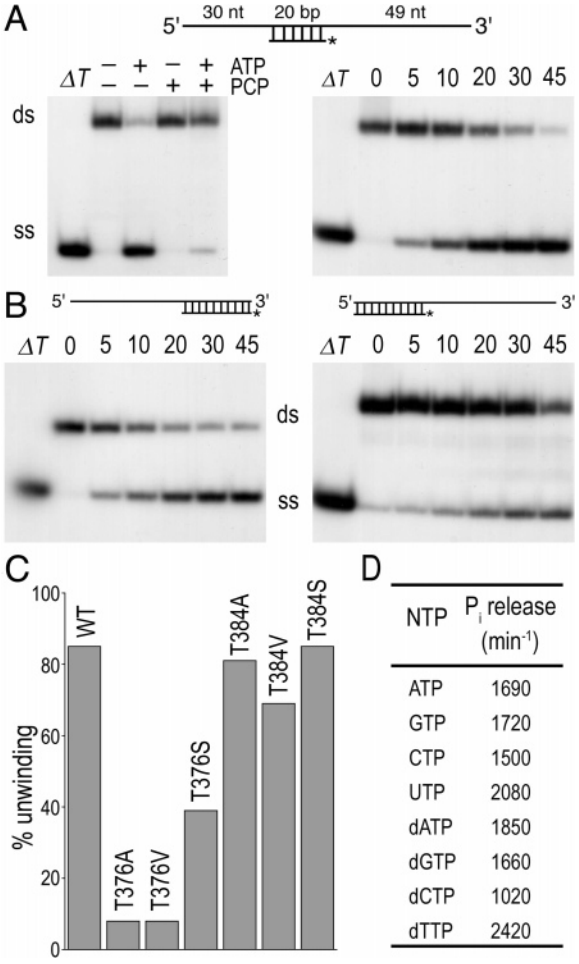

FIGURE 7: Unwinding activity. (A) The helicase substrate, in which a 99 nt RNA strand is annealed to a 20 nt ^{32}P-labeled DNA oligonucleotide, is depicted at the top. Δ*T* shows migration of the labeled DNA oligonucleotide after heating of the substrate for 3 min at 95 °C. Left panel: Reaction mixtures containing 1 μM Prp43 were supplemented (+) with 0.5 mM ATP-Mg (ATP) or 2 mM AMPPCP-Mg (PCP), incubated for 1 h at 37 °C, and analyzed by native PAGE; (−) indicates that ATP-Mg or AMPPCP-Mg was omitted. Right panel: Reaction mixture contained 1 mM ATP-Mg, 1.25 nM helicase substrate, and 1 μM Prp43. Aliquots were withdrawn at the indicated times and halted by addition of SDS-containing loading buffer and transfer to ice. The products were analyzed by native PAGE and autoradiograms of the dried gels are shown. (B) Unwinding of a 5′ tailed 30 bp duplex (left panel), and a 3′ tailed 30 bp helicase substrate (right panel) as a function of time. Reaction mixtures contained 1 mM ATP-Mg, 1 μM wild type Prp43, and 1.25 nM helicase substrate depicted above each panel. (C) Unwinding by mutant proteins. Reaction mixtures containing 1.25 nM 5′/3′ tailed helicase substrate (depicted in panel A), 1 mM ATP-Mg, and 1 μM wild type Prp43 (WT) or the indicated mutant protein were incubated for 1 h at 37 °C. The products were analyzed by native PAGE, and the amounts of ^{32}P-labeled helicase substrate (ds) and single-stranded product (ss) were quantified using a phosphorimager. % unwinding was calculated and the background (incubation in the absence of protein) was deducted in every case. Each datum is the average of two experiments. (D) Prp43 hydrolyzes all common NTPs and dNTPs. Reaction mixtures (100 μL) contained 40 mM Tris-HCl (pH 8), 2 mM DTT, 1 mM NTP-Mg, 0.6 mM poly(A), and 10 nM Prp43. P_i release was measured after incubation for 2−10 min at 30 °C; the values are averages from two measurements.

placed them under the transcriptional control of the *GAL1* promoter on *CEN TRP1* plasmids and introduced them into *PRP43* cells. In parallel, we analyzed strains containing the *GAL1* plasmid, wild type *PRP43*, *T123A*, or the viable motif

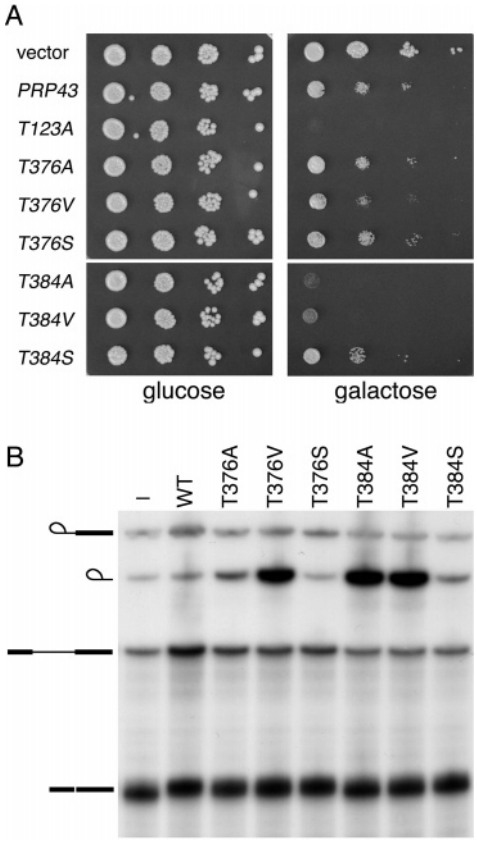

FIGURE 8: (A) Growth inhibition caused by overexpression of lethal Prp43 mutants. Wild type *PRP43* and the indicated mutant alleles under the control of the *GAL1* promoter were transformed into wild type *PRP43* cells. Transformants were grown in liquid cultures (SD-Trp, 2% raffinose). The cultures were adjusted to A_{600} of 10^{-1}, 10^{-2}, 10^{-3}, and 10^{-4}, and 5 μL was spotted to plates containing glucose or galactose (2%) in SD-Trp medium. The plates were photographed after 3 days of incubation at 30 °C. (B) In vitro splicing. Reaction mixtures (10 μL) contained 40% whole cell extract, ∼50 fmol of [^{32}P]GMP-labeled actin precursor RNA, 60 mM potassium phosphate, 2.5 mM $MgCl_2$, 2 mM ATP, and 100 nM of the indicated protein. A control reaction in which buffer and no exogenous Prp43 protein was added is shown in lane (−). The reaction products were resolved by denaturing PAGE and visualized by autoradiography. The symbols at the left indicate the positions of the following labeled RNA species, proceeding from the top to bottom of the gel: lariat-exon 2 intermediate, lariat-intron, pre-mRNA substrate, mRNA.

V mutants *T376S* and *T384S*. All strains grew equally well on glucose-containing medium (Figure 8A). Galactose-induced expression of wild type *PRP43* resulted in slowed growth, insofar as the colonies were smaller than control strains (compare PRP43 and vector) (*18*). The basis for the reduced growth is not known. On galactose-containing medium, the growth of *T376S*, *T384S*, and *T376A* cells was comparable to that of the strain overexpressing wild type *PRP43*. In contrast, galactose-induced expression of T384A and T384V inhibited cell growth, akin to the dominant negative effects elicited by the ATPase-defective T123A mutant. Expression of the lethal T376V mutant slowed growth, indicating that T376V may not compete as well as T384A, T384V, or T123A with wild type Prp43 in vivo. This was not simply due to differences in protein expression, insofar as Western blotting showed that the steady-state levels of mutant Prp43 proteins were similar in each of the strains grown in galactose-containing medium for 6 h (not shown).

Lethal Motif V Mutants Inhibit Spliceosome Disassembly in Vitro. Prior in vitro studies showed that ATPase-deficient Prp43 mutants blocked the release of excised intron RNA from the spliceosome. Whereas released lariats are subjected to debranching and subsequent degradation by enzymes in the splicing extract, the spliceosome-bound lariats are protected from debranching and decay (*18*). Thus, increased lariat intron levels signify a defect in the Prp43-catalyzed release step (*17*−*19*). In the experiment shown in Figure 8B, splicing mixtures containing labeled precursor RNA, yeast whole cell extract and ATP-Mg were supplemented with the various Prp43 proteins (100 nM) and incubated for 15 min at 27 °C. The products were analyzed by denaturing PAGE. mRNA was produced in every case, showing that none of the added Prp43 proteins affected the catalytic steps of pre-mRNA splicing. In the presence of added wild type Prp43 or mutants T376A, T376S, and T384S, the excised lariat intron was released, debranched, and degraded, similar to the unsupplemented reaction. However, when T376V, T384A, and T384S were included in the splicing mixtures, the amount of excised lariat intron increased, indicating a defect in the Prp43-catalyzed release step. We infer that the lethal T376V, T384A, and T384V mutants retain the ability to bind to the spliceosome, but then fail to catalyze intron release. Whereas T376V is probably inactive because of its low ATPase activity (7% of WT), we surmise that the ATPase-proficient T384A and T384V mutants are defective for coupling the energy of ATP hydrolysis to intron release.

Alanine-Scanning Mutagenesis of the C-Terminal Region in Prp43. The peptide motifs that define the DEAH-box family of proteins (*5*, *6*) are located within a central segment (aa 116−430) of the 767 amino acid Prp43 protein (*17*). The conservation in primary structure between Prp43 and other yeast splicing factors Prp2, Prp16, and Prp22 extends beyond the central ATPase/helicase domain into the C-terminal region. The four proteins are ~30% similar over a stretch of 300 amino acids downstream of motif VI (similarities are denoted by ∧ in Figure 9). In Prp43, this segment comprises amino acids 431−720 (Figure 9). Prior deletion analysis had shown that truncating Prp43 at residue 712 abolished its biological function, but Prp43(1−722) was viable (*18*). The C-terminal margin for Prp43 activity (denoted by the arrowhead in Figure 9) coincides with the margin of conservation with Prp2, Prp16, and Prp22 (*21*).

To identify specific side chains within the C-terminal segment (aa 431−720) that were important for Prp43 function, we replaced individual residues or clusters of 2 and 3 residues with alanine. The effects of mutating 97 positions (highlighted in gray in Figure 9) were evaluated by plasmid shuffle. Mutants that grew on 5-FOA were plated to rich medium (YPD) and incubated at 19, 30, and 37 °C. *F445A*, *R459A*, *F480A*, and *F482A* grew as well as wild type *PRP43* at all temperatures, indicating that Phe445, Arg459, Phe480, Phe482 were not important for Prp43 function in vivo (Figure 9). The double-Ala mutants *T441A-E442A*, *L469A-K470A*, *D476A-L477A*, *E497A-L498A*, *L504A-D505A*, *L510A-T511A*, *L513A-G514A*, *L530A-I531A*, *C538A-S539A*, *S550A-V551A*, *V554A-F555A*, *R557A-P558A*, *D566A-D567A*, and *I571A-F572A* and the triple-Ala mutants *P455A-E456A-I457A*, *N461A-L462A-S463A*, *E541A-I542A-L543A*, *K560A-D561A-K562A*, *S654A-G655A-F656A*, *K662A-K663A-R664A*, *V679A-L680A-I681A*, *H682A-P683A-S684A*, *L701A-T702A-S703A*, *N705A-Y706A-I707A*, and *V710A-T711A-S712A* grew as well as wild type at 19, 30, and 37 °C. We surmise that none of the 65 amino acids that were sampled among these 30 Ala-cluster mutants are important for Prp43 function in vivo (denoted by + in Figure 9).

We cannot rule out the possibility that a potential mutational effect at one position might be suppressed by changing the vicinal residue to alanine. However, it appears more likely that changes at neighboring residues exacerbate growth defects, rather than suppress them, a scenario that is exemplified by *F437A-R438A* and *V694A-I695A-Y696A*. Whereas these alanine-cluster mutants did not support growth of the *prp43*Δ strain under 5-FOA selection, the single mutants were viable; *R438A*, *V694A*, *I695A*, and *Y696A* grew as well as wild type cells (denoted by + in Figure 9), and *F437A* exhibited a ts growth defect at 37 °C. Positions at which Ala substitutions resulted in temperature sensitive growth are denoted by * in Figure 9.

P433A-G434A cells failed to grow at 19 °C, but exhibited no growth defect at other temperatures. The mutants *L439A-Y440A*, *F520A-P521A-L522A*, *T544A-I545A-V546A*, *T581A-L582A-L583A*, *N584A-V585A-Y586A*, and *I648A-R649A-K650A* were temperature-sensitive at 37 °C, and *M548A-L549A* and *D578A-H579A-I580A* grew, but formed pinpoint colonies at 37 °C. *W717A-L718A-I719A* cells formed pinpoint colonies at 19 and 30 °C and failed to grow at 37 °C. The severe phenotype caused by eliminating the side chains at aa 717−719 is noteworthy insofar as it approximates the lethality caused by deleting aa 713−722 (bracketed in Figure 9) (*18*).

DISCUSSION

The release of excised lariat intron RNA from the postsplicing complex depends on Prp43's ability to hydrolyze ATP. Here we show that (i) optimal ATP hydrolysis by Prp43 requires an RNA cofactor with a chain length of ≥20 nt; (ii) Prp43 hydrolyzes all common NTPs and dNTPs; (iii) Prp43 can disrupt short nucleic acid duplexes in an NTP-dependent fashion; and (iv) Prp43 binds to RNA with nanomolar affinity. We report that the hydroxyl side chain of Thr384 in motif V is critical for Prp43 function in vivo and for lariat intron release in vitro. However, it is not essential for ATP hydrolysis. These results establish that ATPase activity is not sufficient for Prp43's biological role.

Mutations of DExD/H proteins that abolish in vivo function, yet spare ATPase activity, have been described for yeast eIF4A, Prp2, and Prp22, for vaccinia virus NPH-II, and for the plum pox potyvirus CI protein (*26*, *33*−*37*). It is thought that such mutations impair coupling of the chemical energy from ATP hydrolysis to a conformational step. In the case of Prp22 and NPH-II, the loss of in vivo function correlates with loss of RNA helicase activity, suggesting that the essential conformational step entails disruption of nucleic acid helices (*25*−*27*, *36*). Genetic data suggested that the Prp22 helicase breaks RNA contacts in the spliceosome that involve the U5 snRNP protein Prp8, thereby releasing the mRNA (*26*).

How Prp43 transmits the energy from ATP hydrolysis to intron release is not known. Prp43 exhibits ATP-dependent RNA unwinding activity in vitro; however, this activity does

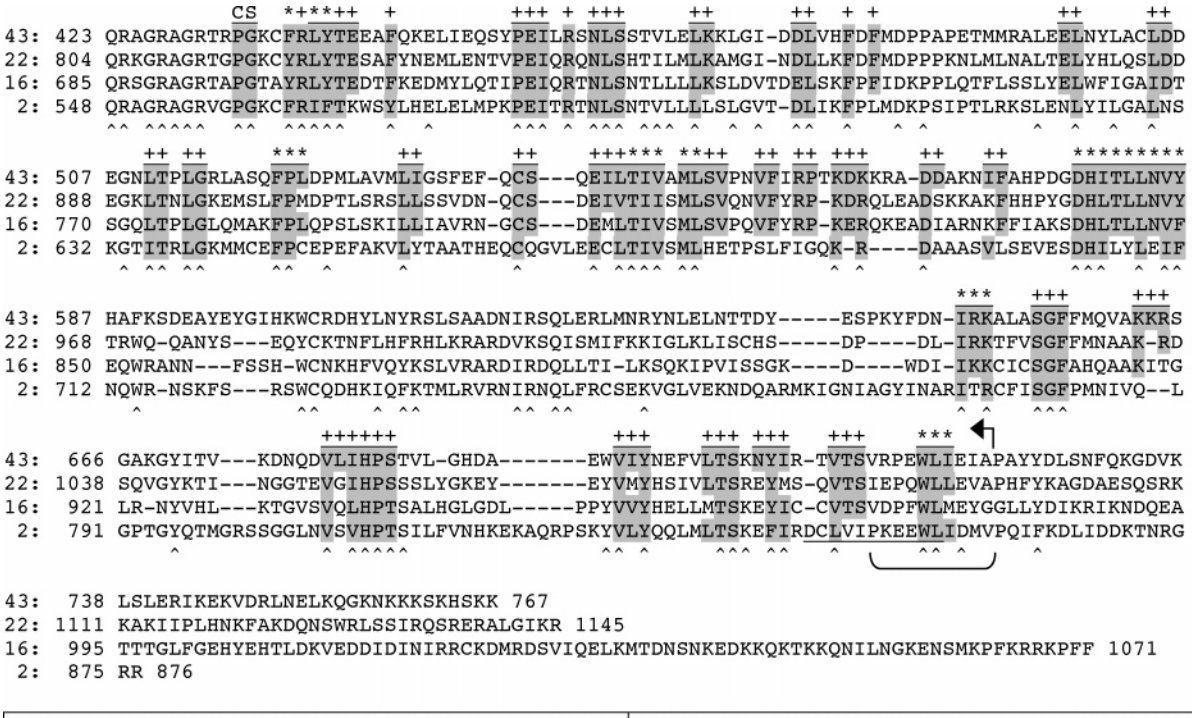

Prp43 mutant	growth	Prp43 mutant	growth
P433A-G434A	*cs*	M548A-L549A	*ts**
F437A-R438A	lethal	S550A-V551A	+++
F437A	*ts*	V554A-F555A	+++
R438A	+++	R557A-P558A	+++
L439A-Y440A	*ts*	K560A-D561A-K562A	+++
T441A-E442A	+++	D566A-D567A	+++
F445A	+++	I571A-F572A	+++
P455A-E456A-I457A	+++	D578A-H579A-I580A	*ts*
R459A	+++	T581A-L582A-L583A	*ts**
N461A-L462A-S463A	+++	N584A-V585A-Y586A	*ts*
L469A-K470A	+++	I648A-R649A-K650A	*ts*
D476A-L477A	+++	S654A-G655A-F656A	+++
F480A	+++	K662A-K663A-R664A	+++
F482A	+++	V679A-L680A-I681A	+++
E497A-L498A	+++	H682A-P683A-S684A	+++
L504A-D505A	+++	V694A-I695A-Y696A	lethal
L510A-T511A	+++	V694A	+++
L513A-G514A	+++	I695A	+++
F520A-P521A-L522A	*ts*	Y696A	+++
L530A-I531A	+++	L701A-T702A-S703A	+++
C538A-S539A	+++	N705A-Y706A-I707A	+++
E541A-I542A-L543A	+++	V710A-T711A-S712A	+++
T544A-I545A-V546A	*ts*	W717A-L718A-I719A	+ *ts*

FIGURE 9: Mutational analysis of Prp43. The sequences of the C-terminal segments beginning at motif VI for Prp43, Prp22, Prp16, and Prp2 are aligned. Amino acids that are identical or similar between the four proteins are indicated by ∧ below the alignment. The 97 residues that were replaced by alanines in Prp43 are highlighted in gray. A line above the sequence indicates that clusters of 2 or 3 residues were replaced by alanines; (+) denotes residues at which alanine replacement elicited no phenotype; (*) marks positions at which alanine replacement resulted in a temperature sensitive phenotype at 37 °C; (*cs*) denotes the 2 vicinal residues at which alanine substitutions caused a growth phenotype at 14 °C. Table: The ability of the mutated *PRP43* alleles to complement a *prp43*Δ strain was tested at 30 °C. Growth of the mutant strains was compared to that of wild type *PRP43* cells on rich medium at 19, 30, and 37 °C. (+++) indicates that the mutant cells grew as well as wild type *PRP43* at all temperatures tested; (+) denotes a mutant that grew more slowly than wild type cells; (cs) indicates that the mutant did not form colonies at 14 °C; (ts) indicates that the mutant did not form colonies at 37 °C; (ts*) means that the mutant formed pinpoint colonies at 37 °C; (lethal) indicates mutants that did not grow at 19, 30, or 37 °C under 5-FOA selection. An 11-aa segment that is important for Prp2's interaction with the spliceosome is underlined (*30*). The C-terminal margin for Prp43 activity is indicated by an arrowhead, and the bracket denotes a 10-aa segment that is important for activity (*18*).

not appear to be a functionally relevant "read-out" for the conformational step catalyzed by Prp43 during intron release, because (i) T376A is viable, yet does not unwind a generic helicase substrate, and (ii) the unwinding activities of the lethal T384A and T384V proteins are not reduced compared to wild type.

The mutational effects on Prp43's inherently feeble unwinding activity mirror those on stable RNA binding, raising the possibility that strand displacement in vitro, which requires a large molar excess of enzyme, occurs when RNA-bound Prp43 hydrolyzes ATP, nudges at the ends of the duplex, and thereby destabilizes it. Such unwinding does not require translocation of the enzyme on single-stranded nucleic acid, which is the defining mechanistic feature of unwinding by several well-characterized directional helicases (*6*).

Members of the DExD/H family of proteins share highly conserved peptide motifs; however, the contribution of individual residues in these motifs to the overall protein function in vivo and in vitro can vary significantly from one DExD/H box protein to another (*38*−*40*). Comparing our mutagenesis results for motif V of Prp43 with those of other DExD/H proteins again underscores that motif conservation does not have clear predictive value for the biochemical properties. Mutations at Thr384 in motif V of Prp43 did not abolish the RNA binding, RNA unwinding, and RNA-dependent ATPase activities. Alanine replacement of the equivalent amino acids in Prp22 (Thr765) and in the PPV CI helicase (Thr313) did not affect RNA binding, but abrogated the RNA helicase activities (*26*, *37*). The T313A mutation in PPV CI also abolished dATP hydrolysis (*37*). The RNA-dependent ATPase activity of Prp22-T765A was undiminished compared to wild type Prp22, but ATP hydrolysis was strictly dependent on an RNA cofactor (*26*). Although the RNA-independent ATPase activity of wild type Prp43 is low (5 min^{-1}), mutations at Thr384 led to a further reduction of the basal ATP hydrolysis (1−3 min^{-1}), concordant with the effects observed for the equivalent Prp22 mutant.

In the crystal structure of hepatitis C virus NS3 helicase bound to $(dU)_8$ oligonucleotide, the motif V Thr411 side chain that corresponds to Thr376 in Prp43 contacts a phosphate in the nucleic acid (*41*). Replacing Thr411 by alanine abolished NS3 helicase activity and the NS3-T411A mutant retained basal ATPase activity, which was slightly increased compared to that of wild type, but was not stimulated by nucleic acid (*42*). Similar effects were observed for the equivalent motif V mutation (T757A) in Prp22 (*26*). Prp43 mutants T376A, T376V, and T376S exhibited increased basal ATPase activity; however, RNA did stimulate ATP hydrolysis, albeit to a lesser extent than wild type.

Ala, Ser, and Val mutations at Thr376 of Prp43 greatly diminished the formation of stable RNA−protein complexes measured by electrophoretic mobility shift assays. Because T376A and T376S were viable and the mutant's affinity for RNA in ATPase stimulation was comparable to that of wild type, stable RNA binding is apparently not essential for in vivo function or for ATP hydrolysis. Moreover, loss of stable RNA binding does not abolish the ability of T376V to compete with wild type Prp43 for spliceosome binding and thereby block intron release. Substitutions at the equivalent motif V residues in Prp22 (T757A) and in HCV NS3 (T411A), which eliminated the responsiveness to a nucleic acid cofactor during ATP hydrolysis, did not affect the RNA binding capacity of Prp22 and reduced that of NS3 by 5-fold (*26*, *42*). Correlating mutational effects on RNA stimulation during ATP hydrolysis with those on direct RNA-binding measurements may be complicated if DExH proteins contain more than one RNA-binding site.

Prp43 shares the ability to hydrolyze all common NTPs and dNTPs with the related DEAH splicing factors Prp2, Prp16, and Prp22 and with the viral DExH helicases NPH-II and HCV NS3 (*43*−*47*). In contrast, DEAD-box proteins use ATP and dATP only, a property that is enforced by the presence of the Q-motif ∼17 aa upstream of motif I (*34*). This peptide motif, which consists of 9 aa including an invariant glutamine and an aromatic residue 16 aa upstream, is uniquely present in the DEAD box subfamily of RNA helicases. Cordin et al. (*48*) demonstrated that the Q motif, which forms extensive interactions with motif I and with the adenine of a bound ADP in the crystal structure of UAP56 (*49*), is indeed involved in ATP recognition and hydrolysis, thereby regulating the RNA binding and helicase activities of Ded1.

Although essential, the role of the ∼300 aa C-terminal segment that is conserved in the DEAH box splicing factors Prp2, Prp16, Prp22, and Prp43 is not well understood. Genetic studies demonstrated that the C-terminal domain of Prp2 contributes to spliceosome binding and truncating the 876-aa Prp2 protein by 42 amino acids inactivates the splicing function of Prp2 without affecting the protein's ATPase activity (*21*). Silverman et al. (*30*) showed that specific mutations in an 11-aa segment near the C-terminus of Prp2 (underlined in Figure 9) ablated spliceosome binding and such mutations also abolished a 2-hybrid interaction between Prp2 and Spp2, an essential splicing factor that is required for association of Prp2 with the spliceosome (*30*, *50*). Spp2 contains a glycine-rich motif (G-patch) found in many RNA binding proteins (*30*, *51*). Genetic data suggest a model in which Prp2 associates with the spliceosome through interaction with the G-patch in Spp2 (*28*). Thus, Spp2 might at least in part determine the specificity for Prp2's interaction with the spliceosome.

A recent report analyzed the association of Prp43 with Ntr1/Ntr2, two essential splicing factors that are required for the release of excised intron during spliceosome disassembly (*19*). Tsai et al. (*19*) showed that Prp43 interacts with the N-terminal region of Ntr1 that contains a G-patch, raising the possibility that, similar to Prp2, Prp43 is recruited to the spliceosome via interaction with a G-patch protein. Whether the C-terminal domain of Prp43 plays a role in spliceosome binding remains to be determined. Our mutational analysis of conserved residues in Prp43 shows that none of the 97 targeted amino acids is essential for Prp43's in vivo function. The alanine scan did, however, identify several *PRP43* alleles that led to conditional growth phenotypes. Conditional phenotypes were elicited by alanine replacements at Pro433/Gly434, Phe437, and Leu439/Tyr440. Their immediate proximity to the essential ATPase/helicase motif VI (*18*) raises the prospect that mutations of these amino acids could affect ATP hydrolysis indirectly by altering the conformation or position of motif VI in the active site.

Mutations of the ^{717}Trp-Leu-Ile^{719} tripeptide, which caused a severe growth defect and lethality at 37 °C, reside within the 11-aa segment that was identified in Prp2 as being important for interaction with Spp2 (underlined in Figure 9) and within the 10-aa segment (VRPEWLIEIA) of Prp43 that defines the C-terminal margin of essentiality (bracketed in Figure 9).

Other mutations that cause temperature sensitive growth defects cluster in segments spanning aa 544−549 (TIVAML)

and 578−686 (DHITLLNVY) of Prp43. Because these peptide motifs are conserved in Prp22, Prp16, and Prp2, it is conceivable that they serve a common function, perhaps as sites for interaction with other spliceosomal components.

ACKNOWLEDGMENT

We thank Dr. Christopher Lima for the generous gift of plasmids.

REFERENCES

1. de la Cruz, J., Kressler, D., and Linder, P. (1999) Unwinding RNA in Saccharomyces cerevisiae: DEAD-box proteins and related families, *Trends Biochem. Sci. 24*, 192−198.
2. Rocak, S., and Linder, P. (2004) DEAD-box proteins: the driving forces behind RNA metabolism, *Nat. Rev. Mol. Cell Biol. 5*, 232−241.
3. Staley, J. P., and Guthrie, C. (1998) Mechanical devices of the spliceosome: motors, clocks, springs, and things, *Cell 92*, 315−326.
4. Gorbalenya, A. E., and Koonin, E. V. (1993) Helicases: amino acid sequence comparisons and structure-function relationships, *Curr. Opin. Struct. Biol. 3*, 419−429.
5. Jankowsky, E., and Jankowsky, A. (2000) The DExH/D protein family database, *Nucleic Acids Res. 28*, 333−334.
6. Tanner, N. K., and Linder, P. (2001) DExD/H box RNA helicases: from generic motors to specific dissociation functions, *Mol. Cell 8*, 251−262.
7. Jankowsky, E., Gross, C. H., Shuman, S., and Pyle, A. M. (2001) Active disruption of an RNA-protein interaction by a DExH/D RNA helicase, *Science 291*, 121−125.
8. Fairman, M. E., Maroney, P. A., Wang, W., Bowers, H. A., Gollnick, P., Nilsen, T. W., and Jankowsky, E. (2004) Protein displacement by DExH/D "RNA helicases" without duplex unwinding, *Science 30*, 730−734.
9. Yang, Q., and Jankowsky, E. (2005) ATP- and ADP-dependent modulation of RNA unwinding and strand annealing activities by the DEAD-box protein DED1, *Biochemistry 44*, 13591−13601.
10. Lorsch, J. R., and Herschlag, D. (1998) The DEAD box protein eIF4A. 2. A cycle of nucleotide and RNA-dependent conformational changes, *Biochemistry 37*, 2194−2206.
11. Schwer, B. (2001) A new twist on RNA helicases: DExH/D box proteins as RNPases, *Nat. Struct. Biol. 8*, 113−116.
12. Von Hippel, P. H. (2004) Helicases become mechanistically simpler and functionally more complex, *Nat. Struct. Mol. Biol. 11*, 494−496.
13. Kim, S. H., and Lin, R. J. (1993) Pre-mRNA splicing within an assembled yeast spliceosome requires an RNA-dependent ATPase and ATP hydrolysis, *Proc. Natl. Acad. Sci. U.S.A. 90*, 888−892.
14. Schwer, B., and Guthrie, C. (1991) PRP16 is an RNA-dependent ATPase that interacts transiently with the spliceosome, *Nature 349*, 494−499.
15. Schwer, B., and Gross, C. H. (1998) Prp22, an RNA-dependent ATPase, plays two distinct roles in yeast pre-mRNA splicing, *EMBO J. 17*, 2086−2094.
16. Wagner, J. D. O., Jankowsky, E., Company, M., Pyle, A. M., and Abelson, J. N. (1998) The DEAH-box PRP22 is an ATPase that mediates ATP-dependent release from spliceosomes and unwinds RNA duplexes, *EMBO J. 17*, 2926−2937.
17. Arenas, J. E., and Abelson, J. N. (1997) Prp43: An RNA helicase-like factor involved in spliceosome disassembly, *Proc. Natl. Acad. Sci. U.S.A. 94*, 11798−11802.
18. Martin, A., Schneider, S., and Schwer, B. (2002) Prp43 is an essential RNA-dependent ATPase required for release of lariat-intron from the spliceosome, *J. Biol. Chem. 277*, 17743−17750.
19. Tsai, R. T., Fu, R. H., Yeh, F. L., Tseng, C. K., Lin, Y. C., Huang, Y. H., and Cheng, S. C. (2005) Spliceosome disassembly catalyzed by Prp43 and its associated components Ntr1 and Ntr2, *Genes Dev. 19*, 2991−3003.
20. Chen, J. H. and Lin, R. J. (1990) The yeast PRP2 protein, a putative RNA-dependent ATPase, shares extensive sequence homology with two other pre-mRNA splicing factors, *Nucleic Acids Res. 18*, 6447.
21. Edwalds-Gilbert, G., Kim, D. H., Silverman, E., and Lin, R. J. (2004) Definition of a spliceosome interaction domain in yeast Prp2 ATPase, *RNA 10*, 210−220.
22. Edwalds-Gilbert, G., Kim, D. H., Kim, S. H., Tseng, Y. H., Yu, Y., and Lin, R. J. (2000) Dominant negative mutants of the yeast splicing factor Prp2 map to a putative cleft region in the helicase domain of DExD/H-box proteins, *RNA 6*, 1106−1119.
23. Hotz, H. R., and Schwer, B. (1998) Mutational analysis of the yeast DEAH-box splicing factor Prp16, *Genetics 149*, 807−814.
24. Schneider, S., Hotz, H. R., and Schwer, B. (2002) Characterization of dominant-negative mutants of the DEAH-box splicing factors Prp22 and Prp16, *J. Biol. Chem. 277*, 15452−15458.
25. Schwer, B., and Meszaros, T. (2000) RNA helicase dynamics in pre-mRNA splicing, *EMBO J. 19*, 6582−6591.
26. Schneider, S., Campodonico, E., and Schwer, B. (2004) Motifs IV and V in the DEAH box splicing factor Prp22 are important for RNA unwinding, and helicase-defective Prp22 mutants are suppressed by Prp8, *J. Biol. Chem. 279*, 8617−8626.
27. Campodonico, E. and Schwer, B. (2002) ATP-dependent remodeling of the spliceosome: Intragenic suppressors of release-defective mutants of Saccharomyces cerevisiae Prp22, *Genetics 160*, 407−415.
28. Wang, Y., and Guthrie, C. (1998) PRP16, a DEAH-box RNA helicase, is recruited to the spliceosome primarily via its nonconserved N-terminal domain, *RNA 4*, 1216−1229.
29. Schneider, S., and Schwer, B. (2001) Functional domains of the yeast splicing factor Prp22p, *J. Biol. Chem. 276*, 21184−21191.
30. Silverman, E. J., Maeda, A., Wei, J., Smith, P., Beggs, J. D., and Lin, R. J. (2004) Interaction between a G-patch protein and a spliceosomal DEXD/H-box ATPase that is critical for splicing, *Mol. Cell. Biol. 24*, 10101−10110.
31. Tanaka, N., and Schwer, B. (2005) Characterization of the NTPase, RNA-Binding, and RNA Helicase Activities of the DEAH-Box Splicing Factor Prp22, *Biochemistry 44*, 9795−9803.
32. Sugimoto, N., Nakano, S., Katoh, M., Matsumura, A., Nakamuta, H., Ohmichi, T., Yoneyama, M., and Sasaki, M. (1995) Thermodynamic parameters to predict stability of RNA/DNA hybrid duplexes, *Biochemistry 34*, 11211−11216.
33. Schmid, S. R., and Linder, P. (1991) Translation initiation factor 4A from Saccharomyces cerevisiae: analysis of residues conserved in the DEAD family of RNA helicases, *Mol. Cell. Biol. 11*, 3463−3471.
34. Tanner, N. K., Cordin, O., Banroques, J., Doere, M., and Linder, P. (2003) The Q motif: a newly identified motif in DEAD box helicases may regulate ATP binding and hydrolysis, *Mol. Cell 11*, 127−138.
35. Plumpton, M., McGarvey, M., and Beggs, J. D. (1994) A dominant negative mutation in the conserved RNA helicase motif 'SAT' causes splicing factor PRP2 to stall in spliceosomes, *EMBO J. 13*, 879−887.
36. Gross, C. H., and Shuman, S. (1998) The nucleoside triphosphatase and helicase activities of vaccinia virus NPH-II are essential for virus replication, *J. Virol. 72*, 4729−4736.
37. Fernández, A., Guo, H. S., Sáenz, P., Simón-Buela, L., Gómez de Cedrón, M., and García, J. A. (1997) The motif V of plum pox potyvirus CI RNA helicase is involved in NTP hydrolysis and is essential for virus RNA replication, *Nucleic Acids Res. 25*, 4474−4480.
38. Hall, M. C., and Matson, S. W. (1999) Helicase motifs: the engine that powers DNA unwinding, *Mol. Microbiol. 34*, 867−877.
39. Bernstein, K. A., Granneman, S., Lee, A. V., Manickam, S., and Baserga, S. J. (2006) Comprehensive mutational analysis of yeast DEXD/H box RNA helicases involved in large ribosomal subunit biogenesis, *Mol. Cell. Biol. 26*, 1195−1208.
40. Granneman, S., Bernstein, K. A., Bleichert, F., and Baserga, S. J. (2006) Comprehensive mutational analysis of yeast DEXD/H box RNA helicases required for small ribosomal subunit synthesis, *Mol. Cell. Biol. 26*, 1183−1194.
41. Kim, J. L., Morgenstern, K. A., Griffith, J. P., Dwyer, M. D., Thomson, J. A., Murcko, M. A., Lin, C. and Caron, P. R. (1998) Hepatitis C virus NS3 RNA helicase domain with a bound oligonucleotide: the crystal structure provides insights into the mode of unwinding, *Structure 6*, 89−100.
42. Lin, C., and Kim, J. L. (1999) Structure-based mutagenesis study of hepatitis C virus NS3 helicase, *J. Virol. 73*, 8798−8807.
43. Kim, S. H., Smith, J., Claude, A., and Lin, R. J. (1992) The purified yeast pre-mRNA splicing factor PRP2 is an RNA-dependent NTPase, *EMBO J. 11*, 2319−2326.
44. Schwer, B., and Guthrie, C. (1992) A conformational rearrangement in the spliceosome is dependent on PRP16 and ATP hydrolysis, *EMBO J. 11*, 5033−5039.

45. Wang, Y., Wagner, J. D., and Guthrie, C. (1998) The DEAH-box splicing factor Prp16 unwinds RNA duplexes in vitro, *Curr. Biol. 8*, 441−451.
46. Shuman, S. (1992) Vaccinia virus RNA helicase: an essential enzyme related to the DE-H family of RNA-dependent NTPases, *Proc. Natl. Acad. Sci. U.S.A. 89*, 10935−10939.
47. Wardell, A. D., Errington, W., Ciaramella, G., Merson, J., and McGarvey, M. J. (1999) Characterization and mutational analysis of the helicase and NTPase activities of hepatitis C virus full-length NS3 protein, *J. Gen. Virol. 80*, 701−709.
48. Cordin, O., Tanner, N. K., Doere, M., Linder, P., and Banroques, J. (2004) The newly discovered Q motif of DEAD-box RNA helicases regulates RNA-binding and helicase activity, *EMBO J. 23*, 2478−2487.
49. Shi, H., Cordin, O., Minder, C. M., Linder, P., and Xu, R. M. (2004) Crystal structure of the human ATP-dependent splicing and export factor UAP56, *Proc. Natl. Acad. Sci. U.S.A. 101*, 17628−17633.
50. Roy, J., Kim, K., Maddock, J. R., Anthony, J. G., and Woolford, J. L., Jr. (1995) The final stages of spliceosome maturation require Spp2p that can interact with the DEAH box protein Prp2p and promote step 1 of splicing, *RNA 1*, 375−390.
51. Aravind, L., and Koonin, E. V. (1999) G-patch: a new conserved domain in eukaryotic RNA-processing proteins and type D retroviral polyproteins, *Trends Biochem. Sci. 24*, 342−344.

BI052656G